PHYSICAL REVIEW C **82**, 067301 (2010)

Half-life of ^{66}Ga

G. W. Severin and L. D. Knutson
Physics Department, University of Wisconsin-Madison, Madison, Wisconsin 53706, USA

P. A. Voytas and E. A. George
Physics Department, Wittenberg University, Springfield, Ohio 45501, USA

(Received 5 November 2010; published 10 December 2010)

We measured the half-life of ^{66}Ga by observing positrons from the β^+ branch to the ground state of ^{66}Zn with a superconducting Wu-type beta spectrometer. Our result is $t_{1/2} = 9.304(8)$ hours, which is the highest-precision measurement to date and disagrees with the Nuclear Data Sheets (NDS) value by over 6σ.

DOI: 10.1103/PhysRevC.82.067301 PACS number(s): 23.40.−s, 29.30.Dn

The nucleus ^{66}Ga decays by electron capture and positron emission to ^{66}Zn with a half-life of more than nine hours, emitting β's up to 4.15 MeV and several γ's with energies exceeding 2 MeV. ^{66}Ga is easy to produce by proton bombardment of natural zinc and is therefore a useful isotope for detector efficiency and energy calibrations [1].

While in the process of carrying out a calibration experiment for a β spectrometer, we noticed that the half-life of ^{66}Ga is significantly shorter than the value quoted in the most recent *Nuclear Data Sheets* evaluation [2], and in light of this, we decided to carry out a dedicated experiment to measure the half-life.

Previous measurements [3–9] of the ^{66}Ga half-life are summarized in Table I. The table also lists the values adopted in the recent evaluations by Woods [10] and by Browne [2]. The values adopted in the two evaluations are not in good agreement.

Our experiment consisted of detecting positrons from the ground-state decay of ^{66}Ga in the Wisconsin Superconducting Beta Spectrometer (WSBS). The WSBS is an iron-free double focusing Wu-type beta spectrometer with a momentum acceptance of roughly 2% full width at half maximum (FWHM) and peak solid angle greater than 0.5 sr [11]. Positrons that pass through the spectrometer are detected with a 10 mm diameter, 5-mm thick Si(Li) detector. The detector has excellent energy resolution for stopped particles (about 10 keV FWHM), and the resulting capability to independently measure the energy of the momentum-selected β's allows for checks on systematic errors in the experiment.

The ^{66}Ga was produced by proton irradiation of a 3 mg/cm^2 natural zinc target. The zinc had been vapor deposited onto a 13-μm thick aluminum foil, mounted on one of the spectrometer source holders. The reaction proceeded as ^{66}Zn(p,n)^{66}Ga with bombardment at 7 MeV using 2 μA of beam for about 30 minutes at the Wisconsin Tandem Accelerator Lab. The target was allowed to sit for one hour to permit short-lived isotopes such as ^{64}Ga and ^{66}Cu to decay to negligible levels. It was then inserted into the counting position of the spectrometer.

Data collection runs were taken at four different WSBS magnet current settings. Two of the settings were used to measure background rates, 0 A which is nonfocusing, and 20 A, corresponding to a beta momentum of 4.96 MeV/c, which is well above the beta decay endpoint as well as the internal conversion electron lines from states in ^{66}Zn. The other two currents, 11 and 14 A, with momenta centered at 2.73 and 3.47 MeV, respectively, were used for decay counting. The choice of relatively high momenta for decay counting helps to reduce the possibility of contributions from contaminants.

Counting proceeded for 52 hours, with around 25 runs completed at each of the four field settings. The individual runs lasted between 200 and 5000 s.

Representative Si(Li) spectra obtained at 11 and 14 A are shown in Fig. 1. The spectra show the distribution of energies that momentum-selected positrons leave in the Si(Li) detector. Counts in the main peaks come from events in which positrons deposit their full energy in the detector, while counts below the peaks correspond to positrons that pass through or scatter out of the detector. The counts above the peak are from events in which one or both of the annihilation γ rays deposit energy in the detector.

For analysis purposes, each spectrum was split into two sections, one encompassing the peak, and one covering the region below the peak as shown in Fig. 1. In this way we can generate four statistically independent measurements of the half-life that have quite different sensitivities to systematic effects such as backgrounds or contaminants. Similarly, electronics effects such as event losses from pileup will have different effects on the counting rates for different summation regions.

The measured counting rates were corrected for background, electronics losses, and gain shifts. The backgrounds were determined by fitting the rate measurements for the 0 and 20 A runs assuming a background with two components, one time independent and one that decayed with the ^{66}Ga half-life. This time-dependent piece was included to account for events in which γ rays from the source scatter inside the spectrometer and deposit energy in the Si(Li) detector. The two background components were roughly equal in magnitude at the start of data collection. The time-independent background rates are listed in Table II. These numbers were consistent between the 0 and 20 A runs, as well as with source-free background runs taken at 11 and 14 A after the conclusion of the experiment.

A systematic shift due to electronics losses (including detector dead time, event pile up, and other signal processing dead time) was also considered. This was modeled with a Monte Carlo simulation that uses measured pulse shapes and

TABLE I. Previous half-life measurements from ^{66}Ga decay, including two evaluations and the result from this work.

Reference	$t_{1/2}$(h)	σ(h)	Data Set
Mann [3], 1937	9.2	0.2	
Henderson [4], 1937	9.4	0.4	
Buck [5], 1938	9.4	0.2	
Rudstam [6], 1956	9.57	0.06	
Carver [7], 1959	9.5	0.1	
Rudstam [8], 1964	9.33	0.08	
Abbas [9], 2006	9.49	0.03	
Browne(NDS) [2], 2010	9.49	0.03	[6–9]
Woods [10], 2004	9.33	0.08	[3,5,7,8]
This work, 2010	9.304	0.008	

time delays in the counting electronics. The net effect is that events are lost from any given summing region of the Si(Li) energy histogram. The losses are proportional to the counting rate and therefore the result can be quoted as a lost time per event. The calculated lost times for regions I through IV are listed in Table II. The correction for the electronics losses shifted the measured half-life value down by 25 s, or about 0.07%.

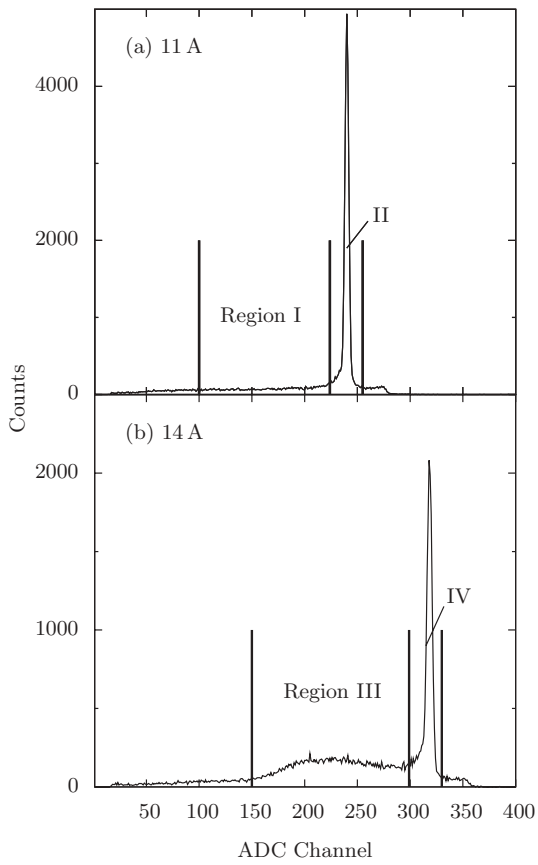

FIG. 1. Representative Si(Li) Spectra for the ^{66}Ga half-life determination, showing the counting regions and defining the labels I, II, III, and IV. (a) An 11 A Si(Li) spectrum, started at 7.4 h after irradiation, with a runtime of 251 s. (b) A 14 A Si(Li) spectrum started at 7.3 h with a runtime of 322 s.

TABLE II. Background rates and electronics losses for ^{66}Ga half-life counting regions.

Region	Background (counts/s)	Electronics Losses (μs/count)	$t_{1/2}$ (h)	χ^2/dof
11 A I	0.0106(30)	0.04	9.284(20)	1.3
11 A II	0.0007(04)	18.1	9.299(12)	1.2
14 A III	0.0072(16)	10.6	9.329(12)	1.0
14 A IV	0.0003(02)	18.2	9.289(13)	0.4

To ensure that the data were not affected by drifts in the Si(Li) electronics gain, the centroids of all of the Si(Li) peaks were tracked throughout the experiment. Corrections to the channel range of the counting regions were applied to account for the small changes in the centroid position over the course of the experiment. These corrections resulted in a change to the final corrected half-life of just 6 s, or about 0.02%.

The background, electronics losses, and gain-shift corrected counting rates for each of the regions are shown in Fig. 2 as a function of time since the start of irradiation. Along with the data is a line representing the best fit to each data set using two parameters, the half-life and an amplitude. Comparing these rates to the values in Table II shows that the corrections applied to the data set are small.

When considering other systematics, we examined the reliability of the clock and the stability of the spectrometer current. Two clocks were used to determine the start times for the runs. One was the internal CPU clock of our data acquisition computer and the other the web-based NIST clock. During the experiment, we observed a monotonic divergence of the two clock readings, ending 7 s apart after 52 hours. This difference is very small compared to the half-life and is negligible compared to the other systematic effects already mentioned. The NIST times were used in the analysis.

The current in the WSBS magnets was also monitored in two ways. The primary measurement was obtained with a

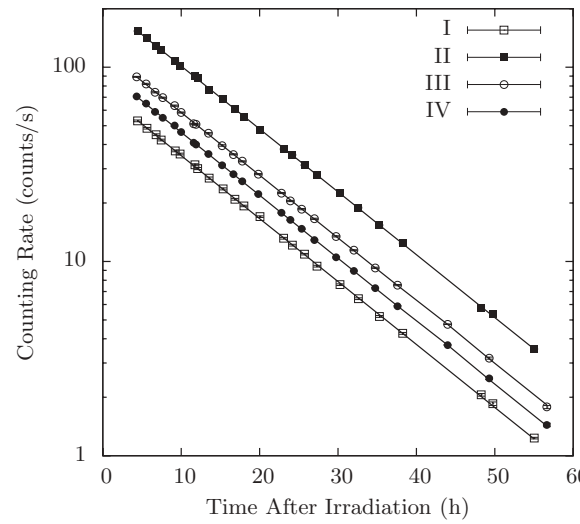

FIG. 2. Decay curves for counting regions in the ^{66}Ga half-life determination. The error bars are smaller than the data points.

Danfysik Ultrastab 867–200i current transducer, which claims to operate with a long-term stability varying less than one part in a million over 1 month. This transducer was used along with a temperature stabilized precision resistor to create a voltage that was monitored with a computer-based analog-to-digital converter (ADC). The measured currents were recorded in an event stream and were also used by a feedback algorithm that produces output signals to regulate the magnet current. A secondary measurement of the current was obtained with a simple shunt resistor monitored with a digital voltmeter. The measured shunt voltages at the repeated currents did not vary by more than three parts in 10^4. A systematic drift in current of that magnitude will affect our half-life measurement at 11 and 14 A by less than 0.05%. Additionally, any drift in our current regulation system will cause shifts at 11 and 14 A in opposite directions due to the slope of the β-momentum spectrum. We observe no significant difference between the half-life measurements at 11 and 14 A, and from this we conclude that the stability of the current does not introduce a significant systematic error.

Least-squares fitting of the data gives a half-life measurement for each of the counting regions from the 11 and 14 A runs. The four half-life values are all in statistical agreement and are listed in Table II. The agreement between the counting regions allows the data set as a whole to be analyzed with a common half-life. To do this, we perform a five parameter fit: one amplitude for each of the four regions and the half-life. The fit achieves $\chi^2 = 92.2$ for 91 degrees of freedom, and the resulting half-life value is $t_{1/2} = 9.304(8)$ h.

TABLE III. Corrections to the measured half-life and the error budget.

Effect	Correction	Error
Statistics	–	24 s
Background	−13 s	3 s
Electronics Losses	−25 s	13 s
Gain Shifts	+6 s	6 s
Total	−32 s	28 s

The error budget for the measurement, along with the impact that the background, electronics losses, and gain-shift corrections had on the final value are listed in Table III. The final uncertainty in $t_{1/2}$ was obtained by combining the statistical error and each of the systematic errors in quadrature. Our new result is the most precise ^{66}Ga half-life measurement to date and the value we obtain is lower than the current NDS half-life by more than six times the uncertainty quoted in that evaluation.

This work is supported in part by NSF Grant No. PHY-0855514.

[1] C. M. Baglin, E. Browne, E. B. Norman, G. L. Molnr, T. Belgya, Z. Rvay, and F. Szelecsnyi, Nucl. Instrum. Methods **481**, 365 (2002).
[2] E. Browne and J. K. Tuli, Nucl. Data Sheets **111**, 1093 (2010).
[3] W. B. Mann, Phys. Rev. **52**, 405 (1937).
[4] L. N. Ridenour and W. J. Henderson, Phys. Rev. **52**, 889 (1937).
[5] J. H. Buck, Phys. Rev. **54**, 1025 (1938).
[6] G. Rudstam, Ph.D. thesis, University of Uppsala, 1956.
[7] J. Carver and G. Jones, Nucl. Phys. **11**, 400 (1959).
[8] G. Rudstam, Nucl. Phys. **56**, 593 (1964).
[9] K. Abbas *et al.*, Appl. Radiat. and Isot. **64**, 1001 (2006).
[10] M. J. Woods and S. M. Collins, Appl. Radiat. Isot. **60**, 257 (2004).
[11] L. D. Knutson, S. L. Cotter, E. A. George, G. W. Severin, and P. A. Voytas (unpublished).